First In-vivo Demonstration of Hologram-assisted Bilateral Blood-Brain Barrier Opening in Non-Human-Primates

Sergio Jiménez-Gambín[†*], Sua Bae[†], Robin Ji[†],, Fotios Tsitsos[†], and Elisa E. Konofagou[†§]
Department of [†]Biomedical Engineering, [§]Radiology, Columbia University, New York City, USA
[*]Email: sj3044@columbia.edu

2023 IEEE International Ultrasonics Symposium (IUS) | 979-8-3503-4645-9/23/$31.00 ©2023 IEEE | DOI: 10.1109/IUS51837.2023.10307955

***Abstract*—Focused ultrasound (FUS) and microbubbles facilitate blood-brain barrier opening (BBBO) non-invasively, transiently and safely, enabling targeted drug delivery into the brain. However, state-of-the-art approaches have not shown the feasibility of simultaneous multifocal BBBO. In this study, we demonstrate for the first time the simultaneous, bilateral BBBO in non-human-primates (NHP) using acoustic holograms in two configurations: targeting caudate and putamen structures. We used a simple and low-cost system composed of a single-element FUS transducer and a 3D-printed hologram, guided by neuronavigation, with a robotic arm. The advantages of holograms are: 1) skull, muscle and brain aberration correction, 2) multiple and highly-localized BBBO with a single sonication, and 3) target-independent positioning of the transducer, defining a promising alternative for time- and cost-efficient therapeutic systems for neurological diseases. Holograms were designed using the k-space method by time-reversal techniques. MRI scans were used for the target and trajectory selection, while CT scans provided the maps for the acoustic properties of skull, muscle and brain. For the BBBO procedure, a robotic arm was used for the transducer positioning allowing positioning errors below 0.1 mm and 0.1 º, and 0.5-0.6-MPa 513-kHz FUS was applied for 4 minutes in conjunction with microbubbles. For BBBO assessment, T1-MRI Post-FUS was acquired. Contrast-enhanced T1-MRI showed bilateral gadolinium extravasation, observing BBBO at both caudate or putamen structures. For the caudate configuration, both BBBO locations were separated by 13.13 mm with a volume of 91.81 mm^3, compared to the simulated separation of 9.40 mm with a volume of 124.52 mm^3. For the putamen configuration, both BBBO locations were separated by 21.74 mm with a volume of 145.38 mm^3, compared to a simulated separation of 22.32 mm with a volume of 156.42 mm^3. No radiological damage was observed. This study demonstrates for the first time the feasibility and safety of hologram-assisted neuronavigation-guided-FUS for simultaneous bilateral BBBO in NHP.**

Keywords—acoustic hologram, blood-brain barrier opening, aberrations correction, low-cost therapy

I. Background

Focused ultrasound (FUS) and microbubbles facilitate blood-brain barrier opening (BBBO) non-invasively, transiently and safely, enabling targeted drug delivery into the brain. State-of-the-art studies based on single-element FUS or phased-array transducers have shown the feasibility of the technique in rodents [1], non-human primates [2], [3] and humans [4], among others studies. However, none of them showed a real-simultaneous, multi-focal, highly-localized BBBO with aberration correction. On the one hand, single-element systems for small animals need a mechanical movement of the transducer for the multi-focal targeting [5]. Several bolus injections of microbubbles are required since they are rapidly cleared from the bloodstream, becoming a time-inefficient approach. The same limitation is found using neuronavigation-guided single-element FUS systems in non-human primates [2], since the mechanical movement of the transducer is a time-limiting factor, in addition to the new injections of microbubbles per each different target. Even though the employment of a robotic arm would considerably reduce the time for each new positioning of the transducer, aberrations would still not be corrected. On the other hand, multi-element devices such as a linear array that provides both FUS and real-time image guidance (i.e., passive acoustic map and B-mode image), show interesting capabilities in both mice [1] and non-human primates [3]. However, simultaneous multi-focal BBBO with aberration correction has not been demonstrated yet. Finally, large aperture multi-element systems for clinical human trials [4] electronically control the amplitude and phase of each piezoelectric element for aberrations correction and focal steering while the transducer remains in a fixed position. However, these systems are limited by their steering angle, high-cost and the requirement for MRI guidance.

To overcome these limitations, holographic acoustic lenses or holograms have shown the transcranial generation of simultaneous multi-focal pressure patterns, acoustic fields matching the focal volume with the geometry of CNS structures, self-bending beams, vortex beams, and simultaneous bilateral BBBO in a mouse brain in vivo [6]-[9]. Acoustic holography has demonstrated therefore to be an excellent alternative, being a low-cost and simple technology. Furthermore, these holograms allow highly-localized targeting of brain structures thanks to the small element size and large amount of them. Moreover, since holograms correct the skull aberrations while providing multi-focusing, a unique sonication and injection of microbubbles is enough for the entire treatment.

State-of-the-art acoustic holographic lensing has shown success in water tanks, through human-skull phantoms, in-vitro NHP and human skulls, and in mice for the BBBO in-vivo, but not in NHP in-vivo. In this study, we demonstrate the feasibility, capability, efficiency and safety of hologram-assisted, highly-localized, bilateral BBBO in NHP for the first time.

II. Materials and Methods

We acquired the 3D geometry and acoustical properties of the skull, brain and surrounding muscle of one NHP from X-ray CT images, and we identified both caudate and both putamen targets from the MRI on Brainsight. Then, we used a single-element FUS transducer, aligned and centered with the NHP's head, and lastly an acoustic hologram was designed and placed in front of the transducer to finally open the blood-brain barrier (BBB) bilaterally.

A. Numerical simulation

We used the pseudo-spectral simulation method with k-space dispersion correction implemented in the acoustic package of the k-Wave toolbox (GPU-optimized) for Matlab [10]. We used a numerical grid with an isotropic spatial step of Δs = 0.48 mm (6 grid points per wavelength), and a Courant-Friedrichs-Lewy number of 0.18 and 0.10 for the time-reversal and forward-propagation simulations, respectively.

B. CT and MRI scans of NHP's head for BBBO planning

We used a CT-scan from one (n = 1) rhesus macaque to model the skull, brain and muscle geometry, with a slice thickness of 0.6 mm and in-slice pixel spacing of 0.35×0.35 mm. The heterogeneous density and sound speed of the skull were converted from Hounsfield units using the linear-piecewise polynomials proposed in [11, 12], and we assumed homogeneous values for brain and muscle [13]-[15]. The absorptions for the skull, brain and muscle were set to 1.39 dB/cm [16], 0.42 dB/cm [14, 15] and 1.0 dB/cm [14], respectively. Note that brain and muscle maps were segmented using the ITK-SNAP software [17].

The T1-weigthed MRI used as planning reference on Brainsight had a spatial resolution of 0.80×0.41×0.41 mm. The 3D contours of caudate and putamen were segmented from this MRI using ITK-SNAP.

C. Hologram design and manufacturing

The heights distribution along the surface of the hologram was obtained by time-reversal technique [18]. In addition, the phase wavefront was unwrapped in order to improve the 3D-printing quality of the hologram [19]. Two virtual sources (one per target structure) were placed at both caudate or putamen regions for the back-propagation step, based on the selected targets on Brainsight. Two additional iterations in simulation were performed in order to equalize the pressures at both foci, due to the different attenuations 1) along each path through the NHP´s head and 2) due to the irregular heights distribution along the surface of the hologram. The amplitude of the left virtual source was adjusted in each iteration as a function of the ratio between the both focal pressures obtained after the forward-propagation simulation in the previous iteration. Both holograms were manufactured after the 3rd simulation for each configuration, made of a 3D-printable resin from Formlabs (ClearResin material, c_H = 2580 m/s, ρ_H = 1171 kg/m^3, α = 1.41 dB/cm [6, 7]).

D. BBBO prodecure, assessment and quantification

Previously to the BBBO procedure, an acoustic calibration was carried out using an ex-vivo NHP skull fragment, submerged in a degassed water tank, to compare the experimentally-measured transcranial attenuation with that of simulationn.

All animal experiments were reviewed and approved by the local Institutional Animal Care and Use Committee prior to all performed studies and were in accordance with the National Institutes of Health guidelines for animal welfare. One male adult rhesus macaque (weight: 14.2 kg, age: 8 y) was sonicated in two separate sessions targeting bilaterally and simultaneously the caudate (session 1) and the putamen (session 2). The NHP was initially sedated with a mixture of ketamine (10 mg/kg) and atropine (0.02 mg/kg) through intramuscular injection. Once sedated, the animal was intubated and catheterized via the saphenous vein. Anesthesia was induced and maintained throughout the experiment using inhalable isoflurane mixed with oxygen (1-2 %).

The single-element FUS transducer used was the Sonic Concepts H-204 (f_0 = 513 kHz, OD = 78 mm, F = 61 mm, and ID = 43 mm) mounted confocally with a passive acoustic mapping (PAM) linear array transducer (Vantage 256, Verasonics) for BBB opening monitoring. This system was attached to a robotic arm (UR5e, Universal Robots), and tracked in 3D, as well as the NHP's head, using a neuronavigation system (Brainsight, Rogue Research). The FUS transducer was driven by a function generator (KeySight 33500B, Santa Rosa, CA, USA) and a power amplifier (A075, ENI Inc., Rochester, NY, USA). A custom coupling cone was designed and 3D-printed to fix the hologram to the transducer, hold the coupling water, and allow the accurate alignment of hologram with Brainsight's calibration plate (also custom-designed and 3D-printed), and therefore with the NHP's head.

Secondly, for the BBBO procedure, 0.05 mL/kg Definity microbubbles were injected intravenously and 513-kHz FUS (0.5 MPa-PNP for caudate and 0.6 MPa-PNP for putamen configuration, PRF: 2 Hz, pulse length: 10 ms) was applied for 4 minutes. T1-weighted MRI scans were acquired before and after intravenous administration of 0.2 mL/kg gadodiamide contrast agent (Omniscan, GE Healthcare Bronk, NY, USA) and post-FUS BBBO was assessed approximately 60 min post-sonication (T1-MRI 3-D spoiled gradient-echo, TR/TE: 20/1.4 ms, flip angle: 30 °, number of excitations NEX: 2, spatial resolution: 500×500 mm, slice thickness: 1 mm with no inter-slice gap) [2]. BBBO was quantified by comparing pre- and post-contrast scans. Safety outcomes were assessed with axial T2-weighted MRI (TR/TE: 3000/80 ms, flip angle: 90 °, NEX: 3, spatial resolution: 400×400 mm, slice thickness: 2 mm with no inter-slice gap) and susceptibility-weighted imaging (SWI; TR/TE: 19/27 ms; flip angle: 15 °, NEX: 1, spatial resolution: 400×400 mm; slice thickness: 1 mm with no inter-slice gap). All scans were performed in a 3-T clinical MRI scanner.

III. Results

Two separate bilateral configurations were studied, firstly targeting the caudate, and secondly the putamen. For the position of the transducer, two aspects were considered: 1) target location independency by keeping it fixed for both cases, and 2) keeping the same focal distance of the single-element transducer without hologram.

A. Caudate configuration

The simulated pressure-field distribution, normalized to the maximum focal pressure, along the coronal and axial planes is shown in Fig. 1 (a1, a2), respectively, where the white contours denote the surface of the transducer, the hologram, the coupling cone, the outer muscle, the skull, the brain and both caudate structures. We observed a bilateral focusing at a focal distance of 60 mm, with a separation distance of 9.4 mm. No focal shifts were observed as the maximum pressure value for each foci was located exactly at the corresponding coordinates of the virtual source, which means that the aberrations were perfectly corrected. The average attenuation for both foci due to the transcranial propagation was 75.94 ± 0.04 %. As our reference calibration measurements were acquired for the configuration of the transducer, without hologram, focusing in free-field, the calculated attenuation in the simulation was relative to this calibration configuration, i.e. relative to the simulation of the single-element transducer in free-field. Finally, the focal volume was defined at the half maximum pressure decay (i.e., 6 dB decay from the maximum pressure)

within the brain (maximum pressure generated at one of the two foci), resulting in 124.52 mm^3.

Next, a target pressure of 0.5 MPa was chosen, with a transcranial attenuation coefficient of 81 %, increased by 5 % from the simulated value (based on an initial calibration of the simulation performed through an ex-vivo NHP skull fragment in a degassed water tank). With these parameters from simulation and thanks to the accurate positioning of the transducer with coupled hologram with respect to the NHP´s head by the employment of the robotic arm, we were able to open the BBB at the caudate bilaterally, verified by the contrast enhancement in Post-FUS T1-MRI along coronal and axial planes, as shown in Fig. 1. (b1, b2), respectively. These two BBBO locations were separated by 13.13 ± 0.41 mm, around 3.7 mm larger than compared to simulation, and their center was shifted by 1.16 ± 0.41 mm to the left direction of the NHP (negative x-axis in Fig. 1.) as compared to the 0.00 mm shift in simulation. The quantified BBBO volume was 100.82 mm^3, from which 91.81 mm^3 was on-target and 9.02 mm^3 off-target. The on-target BBBO volume corresponded to a 74 % of the predicted one provided by the simulation. As Brainsight showed very small positioning errors of ~ 0.1 mm and ~ 0.1 º, the slight discrepancies observed might be due to a registration error for the fiducial markers used to register the NHP's head, as their locations during the MRI scanning for the planning scan might be different than their locations during the treatment session, or due to a registration error for the trajectory of the transducer. In addition, the acoustic properties of the skull, brain and muscle might be slightly different to the actual ones. It might have caused additional slight aberrations which were not considered in the hologram design. Despite all of these, the hologram provided a successful simultaneous bilateral BBBO at both caudate structures, and it was safe as no radiological damage was observed in Post-FUS T2-MRI and SWI scans.

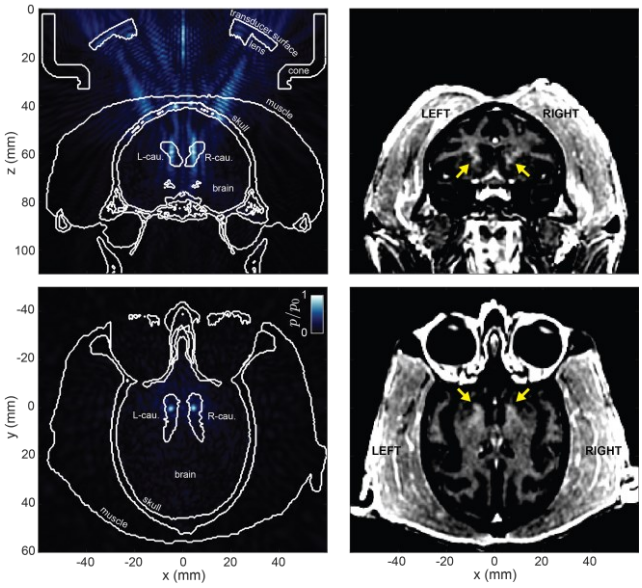

Fig. 1. Hologram-assisted FUS BBBO compared to the simulated pressure-field distribution for the caudate configuration. (a1, a2) Simulated normalized pressure-field distribution along coronal and axial planes, respectively. (b1, b2) Post-FUS contrast enhanced T1-MRI coronal and axial planes, respectively.

B. *Putamen configuration*

A new hologram was designed to target both putamen structures in the two hemispheres. The simulated pressure-field distribution, normalized to the maximum focal pressure, along the coronal and axial planes is shown in Fig. 2 (a1, a2), respectively. We observed a bilateral focusing at 63.5 mm, as the putamen is deeper than the caudate, with a larger separation distance of 22.3 mm. No focal shifts were observed indicating perfect aberration correction. The average transcranial attenuation was 80.49 ± 0.31 % (relative to the simulated transducer without hologram focusing in free-field). Finally, the focal volume defined at the 6 dB decay was 156.42 mm^3.

Next, a derated target pressure of 0.6 MPa was chosen, increased by 0.1 MPa as compared to the caudate configuration, because we expected more shear wave activity due to the stronger steering. We used 85 % for the attenuation compensation (again increasing the simulated one by a 5 %). Then, the Post-FUS T1-MRI along coronal and axial planes, as shown in Fig. 2. (b1, b2), respectively, indicated the contrast enhancement at both putamen structures. These two highest contrast enhancement BBBO locations were separated by 21.74 ± 0.41 mm, showing excellent agreement as compared to simulation, and their center was shifted by only 0.70 ± 0.41 mm to the left direction of the NHP (negative x-axis in Fig. 2.). The quantified BBBO volume was found to be 503.72 mm^3, from which 145.38 mm^3 was on-target and 358.34 mm^3 off-target. The on-target BBBO corresponds to a 93 % of the predicted one, showing an excellent agreement. However, the off-target one was much bigger, located at six separate locations mostly at high vessel density brain regions (such as the middle cerebral artery), and following a particular pattern symmetric from the brain midline. There are three reasons that might explain this discrepancy: 1) Different BBBO pressure thresholds across different brain regions due to tissue inhomogeneities and vessel density, which we have also observed in other BBBO experiments in NHPs [20],

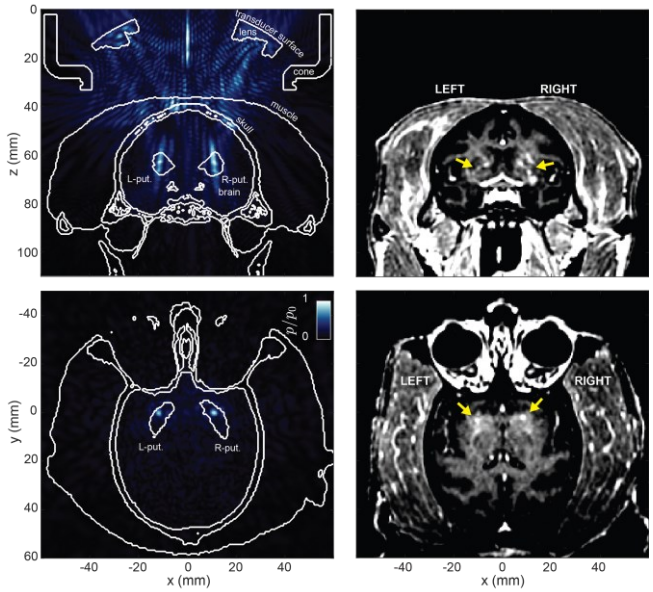

Fig. 2. Hologram-assisted FUS BBBO compared to the simulated pressure-field distribution for the putamen configuration. (a1, a2) Simulated normalized pressure-field distribution along coronal and axial planes, respectively. (b1, b2) Post-FUS contrast enhanced T1-MRI coronal and axial planes, respectively.

[21], in addition to the 0.1 MPa target pressure increase as compared to the caudate configuration, both aspects might have led to the large off-target BBBO volume; 2) The simulation method that we are using assumes negligible shear waves, so on the one hand, the hologram design could not be correcting the phase aberrations completely, and therefore could be improved by performing the time-reversal using an elastic simulation, and on the other hand, the predicted pressure-field distribution might be lacking the generation of relevant side lobes, that we cannot observe in our acoustic simulation result; 3) The aperture of the transducer was not enough to provide two main foci clearly distinguished from off-target lobes.

For this limitation observed, we would recommend using a maximum target pressure of 0.5 MPa for a bifocal targeting configuration using a transducer with a similar size and geometry like the H-204 from Sonic Concepts that we used in this study.

IV. Conclusion

The results reported herein showed the first successful proof of concept of acoustic holograms in non-human primates in vivo for the BBB opening. In particular, the simultaneous, bilateral, localized, and safe BBBO at Parkinson's disease related brain structures, in an efficient manner and being a low-cost approach based on a single-element transducer and a 3D-printed hologram. Moreover, transcranial attenuation was reduced by a 10 % due to the correction of aberrations of the skull, brain and muscle. In addition, the position of the transducer was independent on the target location.

The most relevant limitation found in this study was the noticeable off-target BBBO variability very dependent on slight variations for the target pressure, and it could be improved by employing a larger aperture transducer and elastic simulation models for the hologram design.

The holographic configuration studied here, as a continuation of our study in mice [9], is a proof of concept where the complexity of the focusing pattern is high due to the strong steering, and we expect an improved performance if the hologram is designed to focus at a single spot with less steering or without it, with the potential considerably improve the use of any single-element transducer for aberration correction, while adapting the focal shape to the target structure.

Overall, this work demonstrated the feasibility, capability, efficiency and safety of hologram-assisted FUS for bilateral BBB opening in non-human primates, opening the doors to a novel, powerful and promising approach for low-cost and rapid treatment of brain diseases.

Acknowledgment

This research has been supported by the National Institutes of Health through grants 5R01EB009041 and 5R01AG038961.

References

[1] A. J. Batts, R. Ji, A. R. Kline-Schoder, R. L. Noel, and E. E. Konofagou, "Transcranial theranostic ultrasound for pre-planning and blood-brain barrier opening: A feasibility study using an imaging phased array in vitro and in vivo," IEEE Transactions on Biomedical Engineering, vol. 69, no. 4, pp. 1481-1490, 2021.

[2] A. N. Pouliopoulos, S.-Y. Wu, M. T. Burgess, M. E. Karakatsani, H. A. Kamimura, and E. E. Konofagou, "A clinical system for noninvasive blood–brain barrier opening using a neuronavigation-guided single-element focused ultrasound transducer," Ultrasound in medicine & biology, vol. 46, no. 1, pp. 73–89, 2020.

[3] R. Ji, S. Bae, S. Jiménez-Gambín, A. J. Batts, and E. E. Konofagou, "A Single Linear Array for Simultaneous blood-Brain Barrier Opening and Cavitation Mapping in non-Human Primates," International Ultrasonics Symposium, 2023.

[4] N. Lipsman, Y. Meng, A. J. Bethune, Y. Huang, B. Lam, M. Masellis, N. Herrmann, C. Heyn, I. Aubert, A. Boutet et al., "Blood–brain barrier opening in alzheimer's disease using mr-guided focused ultrasound," Nature communications, vol. 9, no. 1, pp. 1–8, 2018.

[5] M. E. Poorman, V. L. Chaplin, K. Wilkens, M. D. Dockery, T. D. Giorgio, W. A. Grissom, and C. F. Caskey, "Open-source, smallanimal magnetic resonance-guided focused ultrasound system," Journal of therapeutic ultrasound, vol. 4, no. 1, p. 22, 2016.

[6] K. Melde, A. G. Mark, T. Qiu, and P. Fischer, "Holograms for acoustics," Nature, vol. 537, no. 7621, p. 518, 2016.

[7] S. Jiménez-Gambín, N. Jiménez, J. M. Benlloch, and F. Camarena, "Holograms to focus arbitrary ultrasonic fields through the skull," Physical Review Applied, vol. 12, no. 1, p. 014016, 2019.

[8] G. Maimbourg, A. Houdouin, T. Deffieux, M. Tanter and J.F. Aubry, "3D-printed adaptive acoustic lens as a disruptive technology for transcranial ultrasound therapy using single-element transducers," Physics in Medicine & Biology, vol. 63, no. 2, p. 025026, 2018.

[9] S. Jiménez-Gambín, N. Jiménez, A. N. Pouliopoulos, J. M. Benlloch, E. E. Konofagou, and F. Camarena, "Acoustic holograms for bilateral blood-brain barrier opening in a mouse model," IEEE Transactions on Biomedical Engineering, vol. 69, no. 4, pp. 1359-1368, 2021.

[10] B. E. Treeby and B. Cox, "Modeling power law absorption and dispersion for acoustic propagation using the fractional laplacian," The Journal of the Acoustical Society of America, vol. 127, no. 5, pp. 2741–2748, 2010.

[11] U. Schneider, E. Pedroni, and A. Lomax, "The calibration of ct hounsfield units for radiotherapy treatment planning," Physics in Medicine & Biology, vol. 41, no. 1, p. 111, 1996.

[12] T. D. Mast, "Empirical relationships between acoustic parameters in human soft tissues," Acoustics Research Letters Online, vol. 1, no. 2, pp. 37–42, 2000.

[13] F. Duck, "Physical properties of tissues: a comprehensive reference book," Academic press, 2013.

[14] R. S. Cobbold, "Foundations of biomedical ultrasound," Oxford University Press, 2006.

[15] T. Deffieux, and E. E. Konofagou, "Numerical study of a simple transcranial focused ultrasound system applied to blood-brain barrier opening," IEEE transactions on ultrasonics, ferroelectrics, and frequency control, vol. 57, no. 12, pp. 2637-2653, 2010.

[16] G. Pinton, J. F. Aubry, E. Bossy, M. Muller, M. Pernot, and M. Tanter, "Attenuation, scattering, and absorption of ultrasound in the skull bone," Medical physics, vol. 39, no. 1, pp. 299-307, 2012.

[17] P. A. Yushkevich, J. Piven, H. C. Hazlett, R. G. Smith, S. Ho, J. C. Gee, and G. Gerig, "User–guided 3d active contour segmentation of anatomical structures: significantly improved efficiency and reliability," Neuroimage, vol. 31, no. 3, pp. 1116–1128, 2006.

[18] D. Andrés, J. Vappou, N. Jiménez, and F. Camarena, "Thermal holographic patterns for ultrasound hyperthermia," Applied Physics Letters, vol. 120, no. 8, 2022.

[19] M. A. Herráez, D. R. Burton, M. J. Lalor, and M. A. Gdeisat, "Fast two-dimensional phase-unwrapping algorithm based on sorting by reliability following a noncontinuous path," Applied optics, vol. 41, no. 35, pp. 7437-7444, 2002.

[20] S. Bae, K. Liu, A. N. Pouliopoulos, R. Ji, and E. E. Konofagou, "Real-time passive acoustic mapping with enhanced spatial resolution in neuronavigation-guided focused ultrasound for blood-brain barrier opening," IEEE Trans. Biomed. Eng., 2023 (in press).

[21] M. E. Karakatsani, G. M. Samiotaki, M. E. Downs, V. P. Ferrera, and E. E. Konofagou, "Targeting effects on the volume of the focused ultrasound-Induced blood-brain barrier opening in nonhuman primates in vivo," IEEE Trans. Ultrason. Ferroelectr. Freq. Control, vol. 64, no. 5, pp. 798–810, 2017.